FISEVIER

Contents lists available at ScienceDirect

### Materials Science & Engineering A

journal homepage: www.elsevier.com/locate/msea



#### **Short Communication**

# Correlation between hardness and shear banding of metallic glasses under nanoindentation



Fucheng Li<sup>a</sup>, Min Song <sup>a,\*</sup>, Song Ni<sup>a</sup>, Shengfeng Guo<sup>b</sup>, Xiaozhou Liao<sup>c</sup>

- <sup>a</sup> State Key Laboratory of Powder Metallurgy, Central South University, Changsha 410083, China
- <sup>b</sup> Faculty of Materials and Energy, Southwest University, Chongqing 400715, China
- <sup>c</sup> School of Aerospace, Mechanical and Mechatronic Engineering, The University of Sydney, Sydney, NSW 2006, Australia

#### ARTICLE INFO

Article history:
Received 24 December 2015
Received in revised form
15 January 2016
Accepted 16 January 2016
Available online 18 January 2016

Keywords: Hardness Shear banding Softening Hardening Displacement bursts

#### ABSTRACT

Shear banding is an important factor affecting the mechanical properties of metallic glasses. This paper decodes the relationship between hardness and shear banding illustrated by displacement bursts under nanoindentation. Both strain softening caused by shear banding and strain hardening after shear banding contribute to the hardness. It was concluded that randomly distributed large sized displacement bursts lead to more intense straining hardening and therefore a higher hardness increase than the uniformly distributed small sized bursts.

© 2016 Elsevier B.V. All rights reserved.

#### 1. Introduction

In recent years, significant progress has been reached in the development of techniques for probing the mechanical properties of materials on the submicron scale [1-3]. Instrumented indentation, also known as depth-sensing indentation or nanoindentation, has been increasingly used due to the additional levels of control, sensitivity, and data acquisition. Capable of continuously demonstrating load and displacement, indentation load-displacement (P-h) data could provide a wealth of information about the elastic-plastic response of materials [3-15]. Because of these advantages, the indentation response of amorphous alloys has been extensively studied in the last decade [7-17].

It has long been recognized that plastic deformation of metallic glasses (MGs) at room temperature is characterized by strain localization in shear bands [18–21]. In a nanoindentation *P-h* curve, serrated flows or displacement bursts are related to shear banding events [8–10]. Thus, the characteristics of displacement bursts are of significant importance for understanding the elastic–plastic response of MGs. Although a systematic investigation of displacement bursts in MGs under different loading rates has revealed general trends on the effects of loading rate on the number, length, velocity and duration of displacement bursts, the difference between individual datum under the same loading rate is

significant [14]. Hardness, as a commonly used parameter for describing the mechanical behavior of MGs, can easily be obtained by nanoindentation. Different values of hardness can be obtained under the same condition of nanoindentation and were attributed to structural heterogeneity with hard regions surrounded by continuous soft regions in MGs [16]. The structural inhomogeneity results in different numbers and characters of displacement bursts [22]. During plastic deformation under nanoindentation, both strain softening and hardening have been witnessed [23,24]. Creation of free volume during shear banding events leads to strain softening [20], while strong interaction between shear bands and nanocrystals induced within the shear bands during nanoindentation could result in strain hardening [25,26]. Thus, displacement bursts or shear banding events play a key and complicated role in determining the hardness of MGs. The present work aims to understand how shear banding events and the hardness of MGs are mechanistically linked.

#### 2. Experimental

The bulk metallic glass (BMG) studied here is  $\text{Cu}_{36}\text{Zr}_{48}\text{Al}_8\text{Ag}_8$  (atomic percentage) fabricated by arc-melting high-purity copper (99.99 wt%), zirconium (99.7 wt%), aluminum (99.99 wt%) and silver (99.99 wt%) in a Ti-gettered high-purity argon atmosphere using the copper mould suction casting method [27]. The ingot was re-melted four times and stirred using a magnetic beater to ensure the compositional homogeneity. The cylindrical rod with a

<sup>\*</sup> Corresponding author.

E-mail address: msong@csu.edu.cn (M. Song).

diameter of 10 mm and a length of 60 mm was cut into disks with a thickness of  $\sim\!\!2$  mm using a low speed diamond saw under water-cooling. By using a Dmax 2500VB X-ray diffractometer with Cu-K $\alpha$  radiation and a JEOL-2100F transmission electron microscope (TEM), structural characterization of the disks was conducted. Both X-ray diffraction and TEM observations confirmed the amorphous nature of the disks. The disks were mechanically polished to a mirror-like surface and tested using an Ultra nanoindentation tester with a Berkovich diamond tip under the loading control mode. All the nanoindentation tests were carried out under the same condition with a loading rate of 0.01 mN/s and the load limit of 25 mN.

#### 3. Results and discussion

Hardness is calculated from its normal definition:

$$H = \frac{P_{\text{max}}}{A} \tag{1}$$

where  $P_{\text{max}}$  is the peak indentation load and A is the projected area of hardness impression. For a Berkovich indenter, the projected area A is calculated using the Oliver–Pharr method [28]:

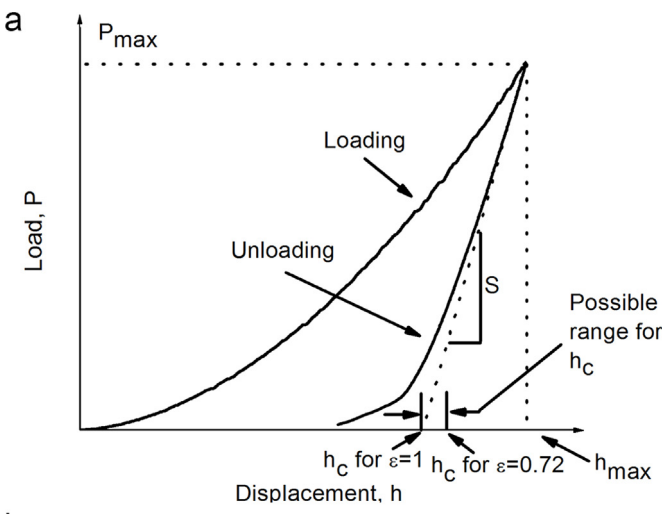
$$A = 24.5h_c^2 \tag{2}$$

$$h_c = h_{\text{max}} - \varepsilon \frac{P_{\text{max}}}{S} \tag{3}$$

where  $h_c$  is the contact depth,  $h_{\rm max}$  is the maximum displacement of indenter,  $\varepsilon$  is a constant that depends on the indenter geometry (For the flat punch,  $\varepsilon=1$ , and for the paraboloid of revolution,  $\varepsilon=0.75$ ) [28], and S=dP/dh is the slope of the initial portion of the unloading curve, which is pure elastic behavior. Thus, for the same sample under the same deformation condition, the value of hardness increases with decreasing  $h_{\rm max}$ . All these corresponding parameters were shown in Fig. 1a.

The hardness distribution from one BMG sample shown in Fig. 1b demonstrates large hardness fluctuation. Similar results have been reported by Wang et al. [16] and Chen et al. [29], which have been suggested caused by structural inhomogeneity of BMGs with isolated hard regions surrounded by continuous soft regions, arising from both initial as-cast samples and deformation induced microstructural evolutions. It was concluded that soft regions enable numerous shear bands to concurrently initiate by rearrangement of free volume or shear transformation zones at different sites to accommodate the applied strain, which intuitively promotes the formation of heterogeneities during the process of plastic deformation [30]. Thus, it is expected that a nanoindentation curve with lower hardness exhibits more displacement bursts.

Fig. 2a shows three P-h curves with different hardness, numbered as curves 1, 2 and 3. It is clear that curves 1 and 2 are close to each other while curve 3 is much deeper with a lower hardness. It is interesting to note that curves 1 and 2 with smaller  $h_{\rm max}$  or higher hardness exhibit more prominent displacement bursts than curve 3. Fig. 2b shows the size distribution of the displacement bursts with the penetrating displacement. It is unambiguous that the displacement bursts in curve 3 are mainly between 0.5–1.5 nm concentrated in the depth higher than 250 nm. However, bursts with much larger size occurred in curves 1 and 2. These larger sized bursts are prominent bursts in Fig. 2a, which are more discrete and random than the bursts in curve 3. Fig. 2c shows the distribution of the size of the displacement bursts. It is obvious that more large-sized bursts can be observed in curve 2 than in



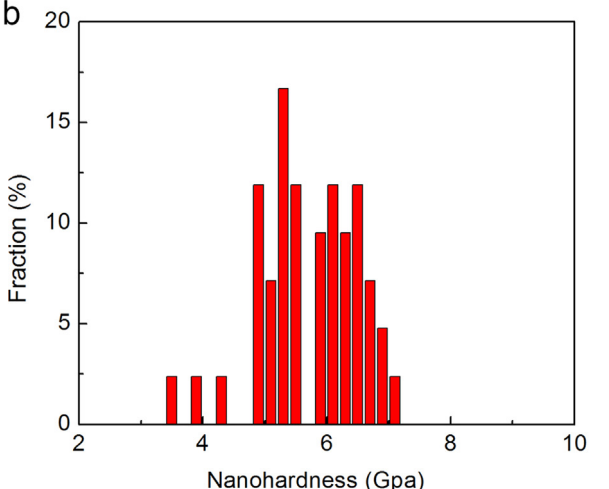


**Fig. 1.** (a) A typical nanoindentation P-h curve and (b) the hardness distribution of a Cu<sub>36</sub>Zr<sub>48</sub>Al<sub>8</sub>Ag<sub>8</sub> BMG.

curve 3. The quantified characteristics of the bursts of the three curves are listed in Table 1. Although the hardness deduced from the three curves are different, the numbers of the bursts are similar. The standard deviations of burst sizes are close to each other for curves 1 and 2. In contrast, the standard deviation for curve 3 is much smaller than for the other two curves. The sums of burst sizes or the accumulated displacement of all bursts in individual curves are also listed. Fig. 2d shows the relationship between the accumulated displacement and the maximum displacement,  $h_{\rm max}$ . It turns out that the accumulated displacement is not the only factor that affects the maximum displacement. Thus, it is difficult to conclude that more bursts will lead to a lower hardness or higher peak displacement, indicating that the relationship between displacement bursts and hardness is complicated.

Under a spherical indenter, it was demonstrated that plastic deformation occurs solely through individual displacement burst [9]. Thus, more displacement bursts will lead to a larger maximum displacement and a lower hardness than those with few bursts. However, under a sharp indenter, plastic deformation can also occur without displacement burst due to the homogeneous flow caused by independent STZs [13,18–20]. The maximum displacement  $h_{\rm max}$  recorded during nanoindentation with a sharp indenter composes roughly three portions: the discrete portion of plastic deformation  $h_{\rm dis}$  that corresponds to displacement bursts, the continuous portion of plastic deformation  $h_{\rm con}$ , and the elastic portion of deformation  $h_{\rm e}$  which will recover during unloading

#### Download English Version:

## https://daneshyari.com/en/article/1573767

Download Persian Version:

https://daneshyari.com/article/1573767

Daneshyari.com